

Interactions, disorder and local defects in graphite

M. A. H. Vozmediano,¹ and F. Guinea², and M. P. Lopez-Sancho²¹ Departamento de Matemáticas, Unidad Asociada CSIC-UC3M, Universidad Carlos III de Madrid, E-28911 Leganes, Madrid, Spain.² Instituto de Ciencia de Materiales de Madrid, CSIC, Cantoblanco, E-28049 Madrid, Spain.
(Dated: April 14, 2024)

Recent experiments report the existence of ferromagnetic and superconducting fluctuations in graphite at unexpectedly high temperatures. The interplay of disorder and interactions in a 2D graphene layer is shown to give rise to a rich phase diagram where strong coupling phases can become stable. Local defects can explain the ferromagnetic signals.

PACS numbers: 75.10.Jm, 75.10.Lp, 75.30.Ds, 71.20.Tx, 73.50.Gr

Introduction. A number of recent experiments suggest that pure graphite behaves as a highly correlated electron system [1]. In particular it shows a metal-insulator transition in magnetic fields and insulating behavior in the direction perpendicular to the planes in different samples [2, 3, 4, 5, 6, 7, 8, 9]. The interest in this material is focussed nowadays in the observation of ferromagnetic behavior [10], enhanced by proton bombardment [11] what opens a new way to the creation of organic magnets.

In refs. [12, 13] a simple microscopic model was proposed as a new framework to study the physics of 2D graphene sheets and its topological variant fullerenes and carbon nanotubes. The main assumption of the model is to neglect the coupling between layers and consider graphite as a pure two-dimensional system. This assumption is supported by experiments where an anisotropy of up to three orders of magnitude is measured in magnetotransport [5]. The model predicts non-Fermi liquid behavior for the graphene system and can account for the linear behavior with energy of the quasi-particle scattering rate [14] observed in photoemission experiments [15].

In this work we review the main features of the model with and without disorder and propose a new mechanism to explain the ferromagnetic fluctuations observed in the experiments.

The model. RG results. The conduction band of graphite is well described by tight binding models which include only the orbitals which are perpendicular to the graphite planes at each C atom [16]. The two dimensional hexagonal lattice of a graphene plane has two atoms per unit cell. A tight binding calculation with only nearest neighbors hopping gives rise to the dispersion relation

$$E(\mathbf{k}) = t \left[1 + 4 \cos^2 \frac{p}{3} k_x + 4 \cos \frac{p}{3} k_x \cos \frac{3}{2} k_y \right] \quad (1)$$

whose lower branch is shown in Fig.1. This dispersion relation gives rise at half filling to a Fermi surface consisting of six isolated points two of which are inequivalent. A low-energy effective Hamiltonian can be defined by expanding the dispersion relation about any of the Fermi points. The resulting Hamiltonian has the form of a massless two dimensional Dirac Hamiltonian. The

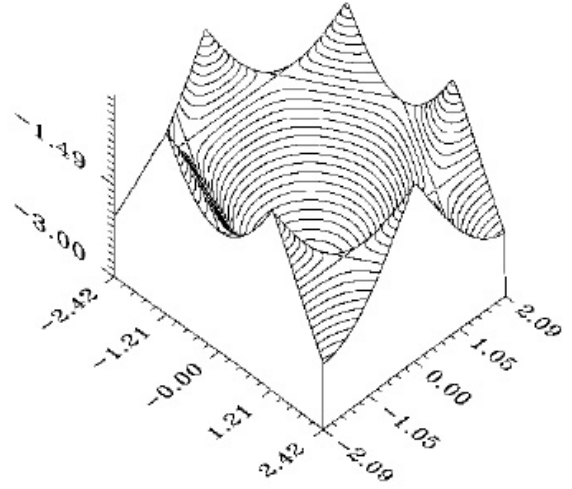


FIG. 1: Lower branch of the electronic dispersion relation. The cusps appear at the six corners of the first Brillouin zone.

Fermi velocity, v_F , can be expressed in terms of the matrix elements between nearest neighbor orbitals, t , as $v_F = (3ta)/2$, where a is the C-C distance.

The electronic states within each graphene plane are described by two two-component spinors associated to the two inequivalent Fermi points in the Brillouin Zone. The Hamiltonian of the free system is:

$$H_0 = i v_F \int d^2x \bar{\psi}(\mathbf{x}) \nabla \cdot \vec{\sigma} \psi(\mathbf{x}) \quad (2)$$

where the two-dimensional matrices are built as appropriate combinations of Pauli matrices [12]. The Hamiltonian (2) gives an effective description of graphite in an energy range bound by a lower cutoff ~ 27 eV dictated by the interlayer coupling, and a higher cutoff, where the bands can no longer be approximated by a linear dispersion relation $\sim 3-4$ eV.

The Hamiltonian (2) is the perfect model for Renormalization Group (RG) calculations. It is scale invariant and does not have the complications of an extended Fermi surface. The model is similar to the $D=1$ electron system in that it has Fermi points and linear dispersion.

Nevertheless naive dimensional analysis shows that four and more Fermi interactions are irrelevant in this two-dimensional case. The only interaction that may survive at low energies is the long (infinite) range Coulomb interaction, unscreened because of the vanishing density of states at the Fermi point. Following the quantum field theory nature of the model, we trade the classical Coulomb interaction

$$H_{ee} = \frac{v_F}{4} \int d^2x d^2x' \bar{\psi}(x) \gamma_0 \psi(x) \frac{g}{|x-x'|} \bar{\psi}(x') \gamma_0 \psi(x') \quad (3)$$

where $g = e^2/4v_F$ is the dimensionless coupling constant, by a local gauge interaction through a minimal coupling.

$$L_{int} = g \int d^2x dt j(x;t) A(x;t); \quad (4)$$

where the electron current is defined as

$$j = (\bar{\psi} \gamma^0 \psi; v_F \bar{\psi} \gamma^i \psi):$$

This interaction is marginal in the RG sense, all the rest are irrelevant. The RG analysis of the model gives the following results [12, 13]:

1. From the computation of the electron self-energy at the one loop level we get a non trivial renormalization of the Fermi velocity that grows in the infrared. This result implies a breakdown of the relation between the energy and momentum scaling, a signature of a quantum critical point.

2. The electron-photon vertex and the photon propagator are not renormalized at the one loop level. This means that the electric charge is not renormalized, a result that could be predicted by gauge invariance, and it also implies that the effective coupling constant $g = e^2/4v_F$ decreases at low energies defining an infrared fixed point of the RG. It is interesting to note that the Lorentz invariance of the model that was explicitly broken by the Fermi velocity is recovered at the fixed point since the velocity of light, c , goes a limit to the growing of the Fermi velocity.

2. From the electron self-energy at two loops order we get a non trivial wave function renormalization meaning that the infrared stable fixed point corresponds to a free fixed point different from the Fermi liquid. This result has been shown to persist in the non-perturbative regime [17]. This is a non-trivial result that has physical implications. In particular it implies that the inverse quasiparticle lifetime increases linearly with energy [14], a result that has been observed experimentally in [15] in the energy range of validity of the model.

In conclusion, we have shown that without disorder, edges, or other perturbations, the graphene system at low energies has gapless excitations differing from the Fermi liquid quasiparticles but does not support magnetic or superconducting instabilities.

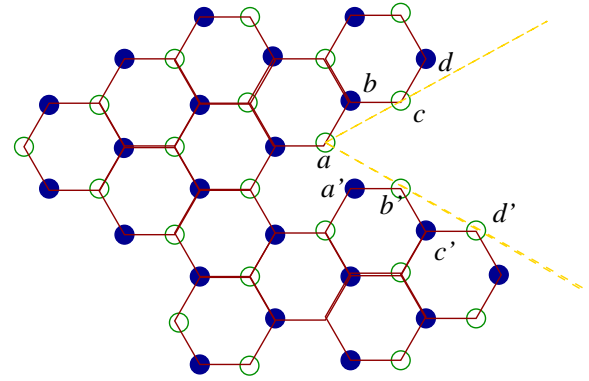


FIG. 2: Formation of a pentagonal ring in the honeycomb lattice. Points $a; b; c; d; \dots$ have to be identified with points $a'; b'; c'; d'; \dots$. The defect can be seen as a disclination, defined by the straight dashed lines.

The strong coupling regime of the graphene system has been analyzed in [18, 19]. There it is argued that a dynamical breakdown of the chiral symmetry (degeneracy between the two Fermi points) will occur at strong coupling and a gap will open in the spectrum forming a kind of charge density wave. Graphite can then be seen as an excitonic insulator that can become ferromagnetic upon doping. Being non-perturbative, these phenomena are likely to be washed out by any amount of disorder at intermediate energies.

Inclusion of disorder.

The previous description analyzes the small momentum scattering due to the long range Coulomb interaction, as it is the only one which leads to logarithmically divergent perturbative corrections. Some electronic instabilities, like ferromagnetism or anisotropic superconductivity, require the existence of short range interactions with significant strength. The irrelevant character of short range interactions can be changed by the presence of disorder that enhances the density of states at the Fermi level.

Disorder can be included in the renormalization group scheme by the introduction of random gauge fields. This is a standard procedure in the study of the states described by the two dimensional Dirac equation associated to random lattices or to integer quantum Hall transitions [20, 21, 22]. There it is seen that, usually, the density of states at low energies is increased. To demonstrate how these gauge fields can arise in the graphene system, we will describe in detail a special type of disorder that we call topological disorder.

The formation of pentagons and heptagons in the lattice, without affecting the threefold coordination of the carbon atoms, lead to the warping of the graphene sheets, and are responsible for the formation of curved fullerenes, like C_{60} . They can be viewed as disclinations in the lattice, and, when circling one such defect, the two sublattices in the honeycomb structure are exchanged (see Fig. 2). The two fermion flavors associated to the two

Fermi points are also exchanged when moving around such a defect. The scheme to incorporate this change in a continuum description was discussed in [17]. The process can be described by means of a non Abelian gauge field, which rotates the spinors in flavor space. The vector potential is that of a vortex at the position of the defect, and the flux is $\Phi = 2$.

Dislocations can be analyzed in terms of bound disclinations, that is, a pentagon and an heptagon located at short distances, which define the Burgers vector of the dislocation. Thus, the effect of a dislocation on the electronic levels of a graphene sheet is analogous to that of the vector potential arising from a vortex-antivortex pair. We can extend this description [23], and assume that a lattice distortion which rotates the lattice axis can be parametrized by the angle of rotation, ϕ , of the local axes with respect to a fixed reference frame. Then, this distortion induces a gauge field such that:

$$A(\mathbf{r}) = 3r \phi(\mathbf{r}) \begin{pmatrix} 0 & i \\ i & 0 \end{pmatrix} \quad (5)$$

Thus, a random distribution of topological defects can be described by a (non abelian) random gauge field.

Other types of disorder can similarly be associated to random gauge fields. The complete Hamiltonian of the system can be written as

$$H = H_{ee} + H_{\text{disorder}} \quad (6)$$

where

$$H_{ee} = \frac{v_F}{4} \int d^2x d^2x' \bar{\psi}(\mathbf{x}) \gamma_0(\mathbf{x}) \frac{g}{|\mathbf{x} - \mathbf{x}'|} \psi(\mathbf{x}') \gamma_0(\mathbf{x}') \quad (7)$$

$$H_{\text{disorder}} = \frac{v}{4} \int d^2x \bar{\psi}(\mathbf{x}) A(\mathbf{x}) \psi(\mathbf{x}) \quad (8)$$

v characterizes the strength and the 4×4 matrix the type of the vertex. In general, $A(\mathbf{x})$ is a quenched, Gaussian variable with the dimensionless variance, i.e.,

$$\langle A(\mathbf{x}) \rangle = 0; \quad \langle A(\mathbf{x}) A(\mathbf{x}') \rangle = \delta^2(\mathbf{x} - \mathbf{x}') : \quad (9)$$

In ref. [24] a complete RG study of the disordered system was analyzed by adding gauge couplings associated to all possible gamma matrices. i) For a random chemical potential, the 4×4 matrix is given by γ_0 . The long range components of this type of disorder do not induce transitions between the two inequivalent Fermi points. This type of disorder yields an unstable fixed line. ii) A random gauge potential involves the 4×4 matrices γ_1 and γ_2 . This type of disorder gives rise to a stable fixed line which is linear in the $(g; \gamma)$ -plane. iii) (a) A fluctuating mass term is described by γ_4 . (b) Topological disorder is given by γ_5 with $\gamma_5 = \gamma_2 \gamma_3$. c) To complete the discussion, we also mention γ_5 where $\gamma_5 = \gamma_2 \gamma_3$. This vertex

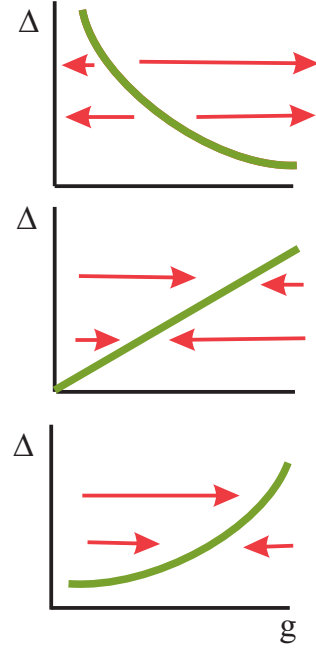


FIG. 3: One-loop phase diagram for two-dimensional massless Dirac spinors including long-ranged electron-electron interaction g and disorder γ . Top: Random chemical potential ($\gamma = \gamma_0$). Center: Random gauge potential ($\gamma = i\gamma_1; i\gamma_2$). Bottom: Random mass term ($\gamma = i\gamma_4$), topological disorder ($\gamma = i\gamma_5$), and $\gamma = i\gamma_5$.

type can be related to an imaginary mass that couples the two inequivalent Fermi points. All these types of disorder will yield a stable fixed line which is cubic in the $(g; \gamma)$ -plane.

The phase diagram obtained in [24] is reproduced in Fig. 3.

i) For a random chemical potential ($\gamma = \gamma_0$), $v = v_1$ remains constant under renormalization group transformation. There is an unstable fixed line at $v_F = v_1^2 = (2e^2)$. In the $(g; \gamma)$ -plane, the strong-coupling and the weak-coupling phases are separated by a hyperbola, with the critical electron interaction $g = e^2/v_F = 2e^4/(v_1^2)$. ii) A random gauge potential involves the vertices $\gamma_1; \gamma_2$. The vertex strength renormalizes as $v = v_F$. There is thus an attractive Luttinger-like fixed point for each disorder correlation strength given by $v_F = 2e^2$ or $g = 2$. iii) For a random mass term γ_4 , topological disorder γ_5 , and $\gamma = i\gamma_5$, we have $v = v_F^2 = v_3$. There is thus again an attractive Luttinger-like fixed point for each disorder correlation strength given by $v_F = \sqrt{3} 2v_3 e^2$ or $g = \sqrt{3} e^4/(2v_3^2)$.

The most interesting phase is the one induced by a random gauge potential, a random mass term or the topological disorder. All of them drive the system towards a new stable, Luttinger-like fixed point. This phase is characterized by a vanishing quasiparticle residue, leading to anomalous one particle properties. The Luttinger

liquid features associated to this fixed line are notoriously difficult to observe, although they can be probed in tunneling experiments, or by measuring the peak width in ARPES. They will also influence the interlayer transport properties [25, 26]. Small perturbations by other types of disorder, like a random local potential induce a flow along this fixed line, as in the absence of interactions [27]. The strong coupling fixed point describes, most likely, a disordered insulating system.

Localized states. In addition to the extended disorder discussed previously, a graphene plane can show states localized at interfaces [28, 29], which, in the absence of other types of disorder, lie at the Fermi energy. Changes in the local coordination can also lead to localized states [30].

The tight binding model defined by the orbitals at the lattice sites can have edge states when the sites at the edge belong all to the same sublattice (zig-zag edges) [28, 29]. These states lie at zero energy, which, for neutral graphene planes, correspond to the Fermi energy.

In a strongly disordered sample, large defects made up of many vacancies can exist. These defects give rise to localized states, when the termination at the edges is locally similar to the surfaces discussed above [31]. Note that, if the bonds at the edges are saturated by bonding to other elements, like hydrogen, the states at these sites are removed from the Fermi energy, but a similar boundary problem arises for the remaining orbitals. A particular simple example is given by the crack shown in Fig. 4].

These states are half filled in a neutral graphene plane. In the absence of electron interactions, this leads to a large degeneracy in the ground state. A finite local repulsion will tend to induce a ferromagnetic alignment of the electrons occupying these states, as in similar cases with degenerate bands [32]. Hence, we can assume that the presence of these states leads to magnetic moments localized near the defects.

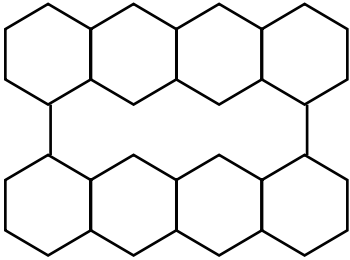


FIG. 4: Example of a crack in a graphene plane. The atoms at the upper edge and those at the lower edge belong to different sublattices.

We now have to analyze the influence of these magnetic moments in conduction band described in the previous sections. The hopping between the states involved in the formation of these moments and the delocalized states in the conduction band vanishes by definition, if the localized states lie at zero energy. Hence, a Kondo like coupling mediated by the hopping will not be induced. The localized and conduction band states, on the other hand, are defined on the same lattice sites. The existence of a finite local repulsion, U , will lead to an effective ferromagnetic coupling. The local coupling, at site i , between the localized states and the conduction band is proportional to $U \sum_j c_{ij} \psi_j$, where ψ_j is charge of state j at site i . In order to get an order of magnitude estimate of the effect of these states, we will assume that the number of states induced near a vacancy is similar to the number of atoms at its edge, N , and that these states are sufficiently localized around the vacancy. Hence, each vacancy nucleates a moment of order N . The effective coupling between a vacancy and the conduction electrons is proportional to UN , and it is distributed over an area N^2 . The conduction electrons will mediate an RKKY interaction between the localized moments:

$$J_{\text{RKKY}}(\mathbf{r}) = U^2 \sum_{\mathbf{r}'} \chi(\mathbf{r}-\mathbf{r}') \chi(\mathbf{r}') = U^2 \frac{a^4}{v_F^2 r^3} \quad (10)$$

Where the static susceptibility is $\chi(\mathbf{k}) / \mathbf{k}^2$ [14], and a is the lattice constant. It is interesting to note that, due to the absence of a finite Fermi surface, the RKKY interaction in eq.(10) does not have oscillations. Hence, there are no competing ferro- and antiferromagnetic couplings, and the magnetic moments will tend to be ferromagnetically aligned, leading to an effective magnetic field, $H_{\text{ext}}(\mathbf{r})$, with non zero average, acting on the conducting electrons.

From power counting, this coupling is relevant in the Renormalization Group sense. Thus, in the presence of extended vacancies, the RG flow discussed in the previous sections has to be arrested at scales comparable to $\hbar H_{\text{ext}}(\mathbf{r}) / U N v_{\text{vac}}$, where v_{vac} is the concentration of the large vacancies which may give rise to localized states. At lower energies, or temperatures, the graphene planes with extended vacancies will behave as a ferromagnet.

Conclusions. In this work we present a microscopic model for studying the low energy properties of a single graphene layer as a model relevant for some graphite samples showing two-dimensional anomalous behavior. In particular we tried to envisage a model able to explain the ferromagnetism observed recently in a variety of graphitic materials.

The model is based on the particular dispersion relation of the 2D honeycomb lattice that, at half filling, has Fermi points instead of Fermi lines. The linearization of the dispersion about a Fermi point gives rise to a model similar to the one-dimensional electron system with zero density of states at the Fermi level. Unlike the 1D case, the real two-dimensional nature of the present model makes the four Fermi interactions irrelevant in

the renormalization group sense while the long range Coulomb interaction is unscreened and plays an important role. It renormalizes the Fermi velocity that grows at low energies while the effective charge is not renormalized, a consequence of the gauge invariance. The effective coupling constant $e^2 = v_F$ goes to zero driving the system to a non-trivial infrared fixed point. As a consequence of the singular Coulomb interaction, the electron acquires an anomalous dimension and the quasiparticle scattering rate grows linearly with frequency at intermediate frequencies, as observed in experiments. The model does not support magnetic or any other short range interactions at this level.

The presence of disorder changes the previous situation in various respects. We have considered two types

of disorder, non-local disorder as the one produced by impurities or lattice distortions, modelled by the coupling of the electrons to random gauge fields as in the random lattice models, and local large defects as the ones produced in the experiments by proton bombardment. Extended disorder gives rise to a rich phase diagram with strong coupled phases whose physical properties are still to be analyzed. Local defects give rise to the appearance of local moments whose interaction can induce ferromagnetism in large portion of the sample.

We thank P. Esquinazi for sharing his experiments with us and for many illuminating discussions. Funding from MCT (Spain) through grant MAT2002-0495-C02-01 is acknowledged.

-
- [1] P. Esquinazi and et al, *Advances in Solid State Physics* 43, 207 (2003).
 - [2] Y. Kopelevich, P. Esquinazi, J. H. S. Torres, and S. Moeckle, *J. Low Temp. Phys.* 119, 691 (2000).
 - [3] P. Esquinazi, A. Setzer, R. Hohne, C. Semmelhack, Y. Kopelevich, D. Spemann, T. Butz, B. Kohlstrunk, and M. Losche, *Phys. Rev. B* 66, 024429 (2002).
 - [4] H. Kempa, P. Esquinazi, and Y. Kopelevich, *Phys. Rev. B* 65, 241101 (2002).
 - [5] Y. Kopelevich, P. Esquinazi, J. H. S. Torres, R. R. da Silva, and H. Kempa, in *Studies of High Temperature Superconductors*, edited by A. Narlikar (Nova Science Pub., Inc, 2003), vol. 45, p. 59.
 - [6] S. Moeckle, P.-C. Ho, and M. B. Maple, *Phil. Mag. Lett.* 82, 1335 (2002).
 - [7] J. M. D. Coey, M. Venkatesan, C. B. Fitzgerald, A. P. Douvalis, and I. S. Sanders, *Nature* 420, 156 (2002).
 - [8] Y. Kopelevich, J. H. S. Torres, R. R. da Silva, F. Morlock, H. Kempa, and P. Esquinazi, *Phys. Rev. Lett.* 90, 156402 (2003).
 - [9] H. Kempa, H. C. Semmelhack, P. Esquinazi, and Y. Kopelevich, *Solid State Commun.* 125, 1 (2003).
 - [10] K. h. Han, D. Spemann, P. Esquinazi, R. Hohne, R. Riede, and T. Butz, *Adv. Mat.* 15, 1719 (2003).
 - [11] P. Esquinazi, D. Spemann, R. Hohne, A. Setzer, K. H. Han, and T. Butz, *Phys. Rev. Lett.* 91, 227201 (2003).
 - [12] J. Gonzalez, F. Guinea, and M. A. H. Vozmediano, *Nucl. Phys. B* 406 [FS], 771 (1993).
 - [13] J. Gonzalez, F. Guinea, and M. A. H. Vozmediano, *Nucl. Phys. B* 424 [FS], 595 (1994).
 - [14] J. Gonzalez, F. Guinea, and M. A. H. Vozmediano, *Phys. Rev. Lett.* 77, 3589 (1996).
 - [15] S. Yu, J. Cao, C. C. Miller, D. A. Mantell, R. J. D. Miller, and Y. Gao, *Phys. Rev. Lett.* 76, 483 (1996).
 - [16] J. C. Slonczewski and P. R. Weiss, *Phys. Rev.* 109, 272 (1958).
 - [17] J. Gonzalez, F. Guinea, and M. A. H. Vozmediano, *Phys. Rev. B* 59, R2474 (1999).
 - [18] D. V. Khveshchenko, *Phys. Rev. Lett.* 87, 246802 (2001).
 - [19] D. V. Khveshchenko, *Phys. Rev. Lett.* 87, 206401 (2001).
 - [20] C. de C. Chamón, C. Mudry, and X.-G. Wen, *Phys. Rev. B* 53, R7638 (1996).
 - [21] H. E. Castillo, C. de C. Chamón, E. Fradkin, P. M. Goldbart, and C. Mudry, *Phys. Rev. B* 56, 10668 (1997).
 - [22] B. Horowitz and P. L. Dussal, *Phys. Rev. B* 65, 125323 (2002).
 - [23] F. Guinea, *Phys. Rev. B* 58, 6622 (1998).
 - [24] T. Stauber, F. Guinea, and M. A. H. Vozmediano (2003), cond-mat/0311016.
 - [25] M. A. H. Vozmediano, M. P. Lopez-Sancho, and F. Guinea, *Phys. Rev. Lett.* 89, 166401 (2002).
 - [26] M. A. H. Vozmediano, M. P. Lopez-Sancho, and F. Guinea, *Phys. Rev. B* 68, 195122 (2003).
 - [27] A. W. W. Ludwig, M. P. A. Fisher, R. Shankar, and G. G. Reinstein, *Phys. Rev. B* 50, 7526 (1994).
 - [28] K. W. Akayabashi and M. Sigrist, *Phys. Rev. Lett.* 84, 3390 (2000).
 - [29] K. W. Akayabashi, *Phys. Rev. B* 64, 125428 (2001).
 - [30] A. A. Ovchinnikov and I. L. Shamovsky, *Journ. of. Mol. Struc. (Theochem)* 251, 133 (1991).
 - [31] F. Guinea, M. P. Lopez-Sancho, T. Stauber, and M. A. H. Vozmediano Work in progress.
 - [32] D. Vollhardt, N. Blümer, K. Held, M. Kollar, J. Schlipf, M. Ulmke, and J. Wahle, in *Advances in Solid State Physics (Weinberg, 1999)*.